Cerebral Cortex, July 2016;26: 3323–3334

doi: 10.1093/cercor/bhw132
Advance Access Publication Date: 11 May 2016
Original Article

ORIGINAL ARTICLE

Celsr3 and Fzd3 Organize a Pioneer Neuron Scaffold to Steer Growing Thalamocortical Axons

Jia Feng[1,2], Quanxiang Xian[1,2], Tingting Guan[1,2], Jing Hu[1,2], Meizhi Wang[1,2], Yuhua Huang[1,2], Kwok-Fai So[1,2,3], Sylvia M. Evans[5], Guoliang Chai[4], Andre M. Goffinet[4], Yibo Qu[1,2,6], and Libing Zhou[1,2,6]

[1]Guangdong-Hongkong-Macau Institute of CNS Regeneration, Ministry of Education CNS Regeneration Collaborative Joint Laboratory, [2]Guangdong key Laboratory of Brain Function and Diseases, Jinan University, Guangzhou 510632, PR China, [3]Department of Anatomy, The University of Hong Kong Pokfulam, Hong Kong SAR, PR China, [4]Institute of Neuroscience, Université catholique de Louvain, Brussels B1200, Belgium, [5]Skaggs School of Pharmacy and Pharmaceutical Sciences, University of California San Diego, La Jolla, CA 92093, USA, and [6]Co-innovation Center of Neuroregeneration, Jiangsu, China

Address correspondence to Libing Zhou, Guangdong-Hongkong-Macau Institute of CNS Regeneration, Jinan University, 601 Huangpu Avenue West, Guangzhou 510632, PR China. Email: tlibingzh@jnu.edu.cn; Yibo Qu, Guangdong-Hongkong-Macau Institute of CNS Regeneration, Jinan University, 601 Huangpu Avenue West, Guangzhou 510632, PR China. Email: tquyibo@jnu.edu.cn

Jia Feng and Quanxiang Xian contributed equally to this work.

Yibo Qu and Libing Zhou contributed equally to this work.

Abstract

Celsr3 and Fzd3 regulate the development of reciprocal thalamocortical projections independently of their expression in cortical or thalamic neurons. To understand this cell non autonomous mechanism further, we tested whether Celsr3 and Fzd3 could act via Isl1-positive guidepost cells. Isl1-positive cells appear in the forebrain at embryonic day (E) 9.5-E10.5 and, from E12.5, they form 2 contingents in ventral telencephalon and prethalamus. In control mice, corticothalamic axons run in the ventral telencephalic corridor in close contact with Isl1-positive cells. When *Celsr3* or *Fzd3* is inactivated in Isl1-expressing cells, corticofugal fibers stall and loop in the ventral telencephalic corridor of high Isl1 expression, and thalamic axons fail to cross the diencephalon–telencephalon junction (DTJ). At E12.5, before thalamic and cortical axons emerge, pioneer projections from Isl1-positive cells cross the DTJ from both sides in control but not mutant embryos. These early projections appear to act like a bridge to guide later growing thalamic axons through the DTJ. Our data suggest that Celsr3 and Fzd3 orchestrate the formation of a scaffold of pioneer neurons and their axons. This scaffold extends from prethalamus to ventral telencephalon and subcortex, and steers reciprocal corticothalamic fibers.

Key words: axon guidance, internal capsule, Isl1, mouse, prethalamus

Introduction

During brain wiring, integrated and protracted mechanisms control axonal growth, fasciculation and branching, target selection, and the formation of appropriate synapses. Guidance of axonal growth cones requires attractive and repellant signals (Tessier-Lavigne 2002) generated by diffusible factors, extracellular matrix molecules and membrane proteins expressed by so-called guidepost cells (Tissir and Goffinet 2013).

The finely organized reciprocal wiring between thalamus and cortex is critical to cortical function (Sherman and Guillery 2011) and results from a tight regulation during development (Lopez-Bendito and Molnar 2003; Molnar et al. 2012). Growing thalamic and cortical axons cross, respectively, the diencephalic–telencephalic junction (DTJ) and the pallial–subpallial boundary (PSPB) before entering a permissive "corridor" in the internal capsule (IC), paved with guidepost cells that assist the progression of axonal growth cones (Lopez-Bendito et al. 2006; Bielle et al. 2011). In addition to guidance by corridor cells, fibers from cortex and thalamus may help each other reciprocally, a mechanism referred to as "handshake" or "rendez-vous" (Molnar and Blakemore 1991; Hevner et al. 2002; Deck et al. 2013). In the corridor, subcerebral cortical projections segregate from corticothalamic axons and are further directed to their targets by additional mechanisms, which include Ryk/Wnt, IGF1, L1-CAM, and Eph/ephrin signaling (Cohen et al. 1998; Dottori et al. 1998; Liu et al. 2005; Ozdinler and Macklis 2006; Greig et al. 2013).

Previous work identified a crucial role for the atypical cadherin Celsr3 and the 7 transmembrane domain receptor Fzd3 in steering cortical and thalamic axons (Wang et al. 2002; Tissir et al. 2005). Conditional inactivation experiments showed that Celsr3 and Fzd3 act via expression in guidepost cells along the pathway, but not in cortical or thalamic neurons themselves (Zhou et al. 2008; Tissir and Goffinet 2013; Hua et al. 2014; Qu et al. 2014). As some cells in the IC corridor express Isl1 transcription factor (Lopez-Bendito et al. 2006), we studied the expression of Isl1, and the wiring phenotype of mice with conditional inactivation of *Celsr3* and *Fzd3* upon Isl1-Cre expression. We show that 2 different pools of Isl1-positive cells are present in the early ventral telencephalon and prethalamus, and that cortical and thalamic axons in the IC corridor run in close contact with them. In Isl1-Cre induced conditional mutants, cortical axons stall and loop after entering the IC corridor, in a more medial position than in *Dlx5/6-Cre;Celsr3*$^{f/-}$ mice, whereas thalamic axons do not cross the DTJ. In control mice, early pioneer axons from ventral telencephalic and prethalamic Isl1-positive cells cross the DTJ in opposite directions prior to the arrival of thalamic fibers. These reciprocal projections and a few intermingled migrating cells form a bridge that provides a substrate for growing thalamic axons. That bridge does not form in *Celsr3* and *Fzd3* mutant mice, accounting for the thalamus nonautonomous derailing of thalamic axons (Qu et al. 2014).

Materials and Methods

Mutant Mice

Animal procedures were approved by the Laboratory Animal Ethics Committee at Jinan University (Permit Number: 20111008001), and adequate measures were taken to minimize pain or discomfort for animals. To produce mice with regional inactivation of *Celsr3*, we crossed *Isl1-Cre;Celsr3*$^{+/-}$ males with homozygous floxed *Celsr3*$^{f/f}$ females to generate *Isl1-Cre;Celsr3*$^{f/-}$ animals; littermates with *Isl1-Cre;Celsr3*$^{f/+}$ or *Celsr3*$^{f/-}$ genotype were used as controls. A similar strategy was used for regional inactivation of *Fzd3*. *Isl1-Cre;Celsr3*$^{f/-}$ and *Isl1-Cre;Fzd3*$^{f/-}$ mice are weak and have frequent hindlimb paresis, and most die around P21 (Chai et al. 2014). *Rosa26*^{Tomato} and *Rosa26*^{YFP} mice were crossed with *Isl1-Cre* mice to trace Cre-expression. The *Thy1-YFP* transgene was used to trace subcerebral tracts (Feng et al. 2000). *Dlx5/6-Cre* mice (Stenman et al. 2003) were used to compare distribution of Dlx5/6- and Isl1-positive cells.

Immunohistochemistry

Immunohistochemistry was carried out using the following antibodies: mouse anti-Calbindin (CB, 1:3000, Sigma), rabbit anti-Calretinin (CR, 1:400, Invitrogen), mouse anti-Reelin (Reln, G10, 1:2000, provided by AMG), rabbit anti-Pax6 (1:200, Covance), mouse anti-neurofilament (NF; 2H3,1:500, Hybridoma bank), mouse anti-Isl1 (39.4D5, 1:500, Hybridoma bank), rabbit anti-Isl1 (1:2000, Abcam), goat-anti cleaved Caspase3 (1:500, bcam), goat-anti-choline acetyltransferase (ChAT, 1:100, Millipore) and rat-anti Fzd3 (1:400, R&D). Cortical barrels were studied in vibratome sections of flattened cortex, stained with guinea pig anti-Vglut2 (1:2000, Millipore). Signal was detected with an anti-mouse/rabbit universal ABC kit (PK-6200, Universal, Vector) or the following fluorescent secondary antibodies: donkey anti-mouse Alexa fluor 546 (1:1000, Invitrogen), donkey anti-mouse Alexa fluor 488 (1:1000, Invitrogen), donkey anti-rabbit Alexa fluor 488 (1:1000, Invitrogen), donkey anti-rabbit Alexa fluor 546 (1:1000, Invitrogen), goat anti-guinea pig Alexa fluor488(1:1000, Invitrogen).

DiI and NeuroVue Tracing

E13.5 and P0 brains were fixed with 4% paraformaldehyde (PFA) overnight at 4°C. Small DiI crystals (D3911, Molecular Probes) were inserted in the thalamus or cortex using a tungsten needle. To trace pioneer axon projections, we prepared vibratome sections of E12.5 brains and implanted NeuroVue (24 837, NeuroVue Jade, Polysciences) or DiI in prethalamus or ventral telencephalon. To trace early thalamocortical axons, we prepared 600-µm thick oblique vibratome sections of E13.5 brains and implanted NeuroVue in dorsal thalamus. After incubation in phosphate buffer saline (PBS) containing 0.08% NaN_3 at 37°C for 1–3 weeks, samples were cut (vibratome, 80 µm thickness) and observed under fluorescence microscopy.

Slice Culture and Neuron Tracing

Rosa26^{Tomato} females were crossed with *Isl1-Cre* males and plugs were checked in the morning, scored as E0.5. Slice culture was carried out as reported (Zhou et al. 2007). Briefly, brains from E12.5 embryos were rapidly removed on ice and *Isl1-Cre;Rosa26*^{Tomato} brains were selected under a fluorescence dissection microscope. Brains were embedded in 4% low melting agarose (1273c458, Amresco), and sectioned into 400-µm thick, oblique sections with a vibratome (MA752, Campden, USA). Selected sections containing prethalamus and ventral telencephalon were cultured in 12-well plates, in Dulbecco's modified Eagle's medium/F12 (DMEM-F12, 1 747 275, Gibco by Life Technologies) supplemented with B27 (1/50), G5 (1/100), and penicillin (1/1000) (all from Invitrogen). After recovering for 1 h at 37°C in the incubator, slices were positioned under a dissection microscope and small pieces of filter paper immersed in 10 µM CellTracker™ Green (CMFDA, c7025, Life Technologies) were inserted into the prethalamus or ventral telencephalon using a tungsten needle. Slices were returned to the incubator and cultured for 2 days. They were fixed with 4% PFA for 2 h at 4°C in the dark and mounted on slides after several washings in PBS. Images were captured with a confocal microscope (Zeiss LSM 780, Germany).

Immunoelectron Microscopy

E13.5 brains were fixed in a solution containing 0.3% glutaraldehyde, 15% picronitric acid, and 4% PFA in 0.1 M phosphate buffer (pH 7.4), overnight at 4°C, and cut into 40–50 µm coronal sections using a vibratome. After rinses in PBS (pH 7.4), sections were treated with 1% $NaBH_4$ and 0.3% H_2O_2 for 30 min, blocked with 0.5% bovine serum albumin and incubated with primary antibodies (mouse anti-NF and rabbit anti-Isl1) at 4°C overnight. Signal was detected with an ABC kit (PK-6200, Universal, Vector). Regions of interest were cut into ~1-mm blocks which were treated with 1% osmium tetroxide and 1% uranylacetate, and embedded in EMbed 812 (Electron Microscope Sciences). Thin sections were stained with 2% uranyl acetate for 30 min and 1% lead citrate for15 min. Images were captured with a Philips 400 electron microscope.

In Situ Hybridization

Celsr3 digoxigenin-labeled riboprobes were prepared and used as described previously (Tissir et al. 2004). Briefly, E12.5 and E13.5 embryos were fixed in 4% PFA in PBS, cryoprotected in sucrose, and 20-µm thick cryostat sections were prepared under RNAse-free conditions. Sections were treated with 1 µg/mL Proteinase K (P-6556, Sigma) for 10 min, acetylated with 0.1 M triethanolamine/0.25% acetic anhydride for 15 min, washed, placed in prehybridization solution at 60°C for 4 h, and hybridized with 1.2 µg/mL probe at 60°C for 16–20 h. Signal was detected with anti-digoxigenin antibody (1:800, Roche) and visualized by NBT/BCIP staining.

Isl1 and Fzd3 RNAscope

E12.5 brains were dissected out in PBS, embedded with cryo-embedding medium (OCT) and frozen immediately on dry ice. Sixteen micrometer thick frozen sections were fixed in 4% PFA for 15 min at 4°C, dehydrated in serial ethanol (50%–70%–100%–100%–100%), each for 5 min, and processed according to the protocol provided in the RNAscope® kit (Advanced Cell Diagnostics. INC, Cat. 320 293). Briefly, after pretreatment with the prehybridization solution for 20 min at room temperature, the sections were hybridized with mixed probes of Isl1 and Fzd3 mRNA, for 2 h at 40°C. After 4-step amplification, the sections were counterstained with DAPI. All solution and probes are provided in the RNAscope® kit. The images were captured with a confocal microscope (Zeiss LSM 780, Germany).

Confocal and 2-Photon Microscopy

Confocal sections were made using a Zeiss LSM 700 or 780 and deconvolved using AutoQuantX (Media Cybernetics, USA) to improve the signal-to-noise ratio. A 2-photon microscope (Zeiss LSM 780) was used to prepare stacks of optical sections at 1 µm intervals in the region of the DTJ, and movies were generated using the Imaris software.

Results

Isl1-Positive Cells Develop Early in Ventral Telencephalon and Prethalamus

Thalamocortical axons are guided by corridor cells in the IC, some of which express Isl1 and originate from the lateral ganglionic eminence (LGE) (Lopez-Bendito et al. 2006). However, when *Celsr3* is inactivated in Gsh2-positive LGE progenitors (Corbin et al. 2003), no abnormal axonal bundles are found in the IC (Zhou et al. 2008), indicating that Celsr3 is not crucial for the function of LGE derived corridor cells or that some Isl1 guidepost cells originate from other sources than the LGE. To define better the localization and developmental history of Isl1-positive cells in the forebrain, we used Isl1 immunohistochemistry and *Isl1-Cre;Rosa26*^{Tomato} mice. The first Isl1-positive cells were seen at the ventral aspect of the early diencephalon at E9.5-E10.5 (Fig. 1*A1–B2,I*). At E11.5, additional cells were found rostrally in the ventral telencephalon, and more caudally in the diencephalic region (Fig. 1*C1–D2,I*). This pattern was better defined at E12.5 and E13.5, with increasing numbers of Isl1-positive cells in ventral telencephalon, and segregation of 2 contingents in the diencephalon, a dorsal one in prethalamic areas (see below), and another one in the hypothalamic anlage, which will not be mentioned further (Fig. 1*E1–H2,I*). Unlike those in telencephalon, all Isl1-positive cells in the prethalamic region were Pax6 positive. They were negative for Reelin (Reln), Calretinin (CR), and Calbindin (CB) (Fig. 2), showing that they did not correspond to the thalamic eminentia, which is CR positive (Abbott and Jacobowitz 1999), nor to the zona limitans intrathalamica (also called "central diencephalic organizer"), which is Pax6-negative (Caballero et al. 2014). They also differed from the Reln-positive "reticular" thalamus, including zona incerta and ventral lateral geniculate nucleus (Schiffmann et al. 1997). The localization and marker expression of those Isl1-positive cells fitted best with their belonging to the prethalamus, a derivative of prosomere 3 (p3) (Vue et al. 2007; Scholpp and Lumsden 2010; Inamura et al. 2011).

As Celsr3 is required in guidepost cells that express Dlx5/6 (Zhou et al. 2008), we compared the distribution of Isl1- and Dlx5/6-positive cells, using Isl1 immunohistochemistry and EGFP expression from the *Dlx5/6-Cre-EGFP* transgene (Stenman et al. 2003). At E10.5, Isl1 was expressed at the midline, and EGFP laterally to the Isl1-positive region, with little overlap; some EGFP-positive cells were located in the ventral telencephalon where no Isl1-positive cell could be seen (see Supplementary Fig. 1*A–C*). At E13.5, Isl1-positive cells were abundant in the central tier of the ventral telencephalon, whereas the peak of EGFP expression was in the dorsolateral tier (see Supplementary Fig. 1*D–F*). At that stage, some Isl1-positive cells in the IC region were also EGFP-positive (see Supplementary Fig. 1*G–I*). In the diencephalon, the distribution of EGFP-positive cells was wider than that of Isl1-positive cells (see Supplementary Fig. 1*F*). Most Isl1-positive cells in prethalamus were EGFP-positive, whereas dorsally located EGFP-positive cells did not express Isl1 (see Supplementary Fig. 1*J–L*). Previous in situ hybridization (ISH) studies showed that *Celsr3* and *Fzd3* mRNA are widely expressed in ventral telencephalon and prethalamus. To confirm coexpression of Fzd3 and Isl1 proteins in the prethalamus and ventral telencephalon, we used IHC. As shown in Supplementary Figure 2*A–D*, at E12.5 most Isl1-positive cells were positive for Fzd3. The cellular colocalization of Fzd3 and Isl1 mRNAswas also shown using RNAscope (see Supplementary Fig. 2*E–H*).

In mice, the first thalamocortical and corticothalamic axons respectively reach the medial and lateral aspects of the ventral telencephalon around E13.5 and then progress rapidly in the corridor. To see whether Isl1-positive cells are closely apposed to growing axons and therefore qualify as candidate guidepost cells, we examined the region of the IC corridor using DiI tracing to label corticofugal axons, and *Isl1-Cre;Rosa26*^{YFP} mice to label Isl1-positive cells. DiI-labeled axons ran almost parallel to one another and came in close contact with Isl1-positive cells (Fig. 3*A*), which was confirmed by NF and Isl1 double immunostaining (Fig. 3*B*). We then immunostained vibratome sections

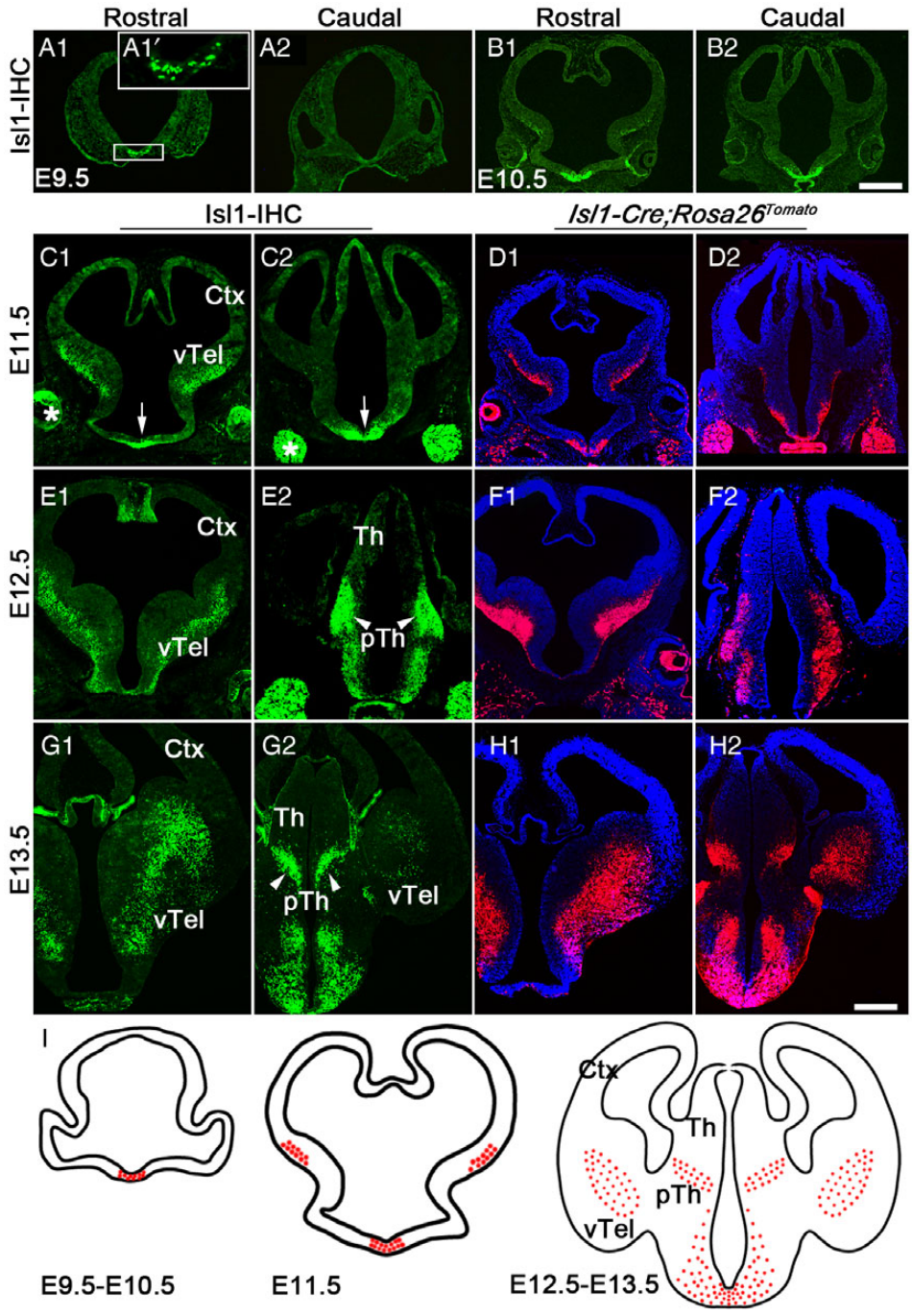

Figure 1. Development of Isl1-positive cells in forebrain. Isl1 expression was studied using anti-Isl1 immunohistochemistry (*A*, *B*, *C*, *E*, and *G*) and by mapping tomato fluorescent protein expression using *Isl1-Cre;Rosa26*^{Tomato} mice (*B*, *D*, *F*, and *H*). Inset in A1 (A1′) is a magnification of the boxed area. (*A* and *B*) Isl1-positive cells appeared at E9.5–E10.5, close to midline. (*C* and *D*) At E11.5, cells expressing Isl1 and tomato protein appeared in ventral telencephalon (vTel) and hypothalamic anlage (arrows). (*E*–*H*) At E12.5 (*E* and *F*), the number of Isl1-positive cells increased in ventral telencephalon and hypothalamic anlage, and another population appears in the prethalamic region (pTh, arrowheads), a pattern that became better defined at E13.5 (*G* and *H*). I: schematic summary of development of Isl1-positive cells. *, trigeminal ganglion. Th, thalamic anlage; Ctx, cortex; IHC, immunohistochemistry. Scale bars: 400 μm.

with mouse anti-NF and rat anti-Isl1 antibodies, detected signal with diaminobenzidine, and observed the distribution of the precipitate by electron microscopy. As shown in Figure 3*C*, NF-positive axons were found in direct contact with the surface of Isl1-positive cells, identified by their immunopositive nuclei. These results suggest that Isl1-positive cells in the IC are in a position to interact directly and serve as guidepost to axons of cortical and presumably thalamic origin.

What could be the fate of early Isl1-positive guidepost cells? To answer this question, we combined lineage tracing using *Isl1-Cre* and the *Rosa26*^{Tomato} transgene, with IHC for the ventral telencephalic marker ChAT, and the apoptosis marker activated (cleaved) Caspase3. We examined ventral telencephalic areas at E15.5, P0, P5, and P10. ChAT immunoreactivity was detected in almost all cells from the Isl1 lineage from P5 onward, whereas activated Caspase3 immunoreactivity was very low, almost

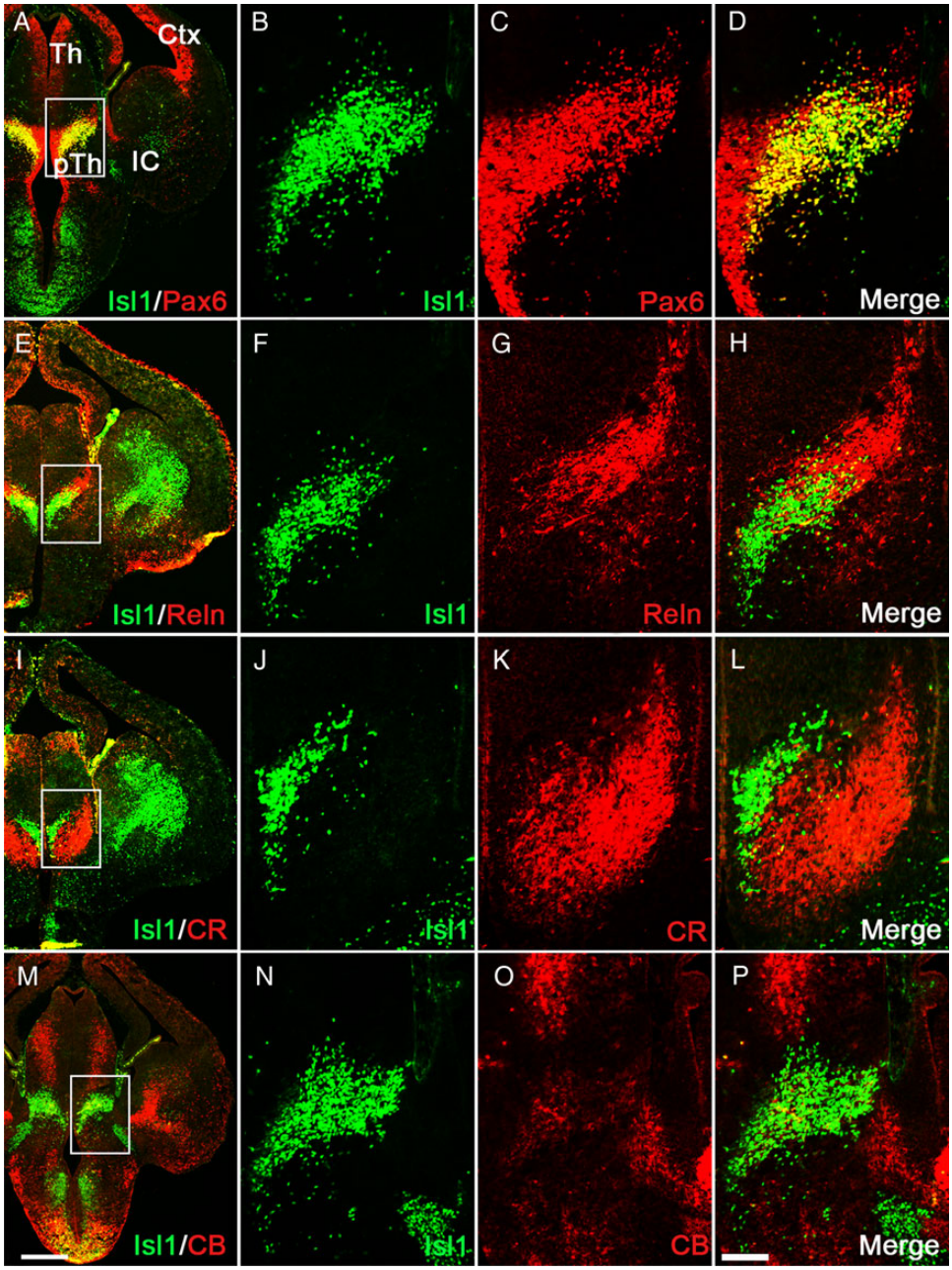

Figure 2. Isl1-positive cells in the prethalamic region are positive for Pax6 and negative for Reln, Calretinin, and Calbindin. (*A–D*) E13.5 sections double-stained by Pax6 and Isl1. In the prethalamic region, the distribution area of Pax6-positive cells was wider than that of Isl1-positive cells (*B* and *C*) and almost all Isl1-positive cells were Pax6-positive (*D*). (*E–H*) Double staining for Isl1 and Reln. Isl1-positive cells were consistently negative for Reln, indicating that they do not belong to the reticular thalamus. (*I–P*) Double staining for Isl1 and Calretinin (CR) or Calbindin (CB) showed no colocalization, suggesting that Isl1-cells are not part of the thalamic eminences. Ctx, neocortex; Th, thalamus; IC, internal capsule; pTh, prethalamus. Scale bars: 400 μm (*A*, *E*, *I*, and *M*); 100 μm (*B–D*, *F–H*, *J–L*, and *N–P*).

undetectable at all stages studied (see Supplementary Fig. 3). Those results indicate that most early born Isl1 cells, presumably including guidepost cells, do not undergo apoptosis and differentiate in cholinergic and possibly some other types of neurons in the postnatal period.

Corticothalamic and Corticospinal Projections are Defective in *Isl1-Cre;Celsr3*$^{f/-}$ Mice

Inactivation of *Celsr3* upon Isl1-Cre expression was validated previously in E12.5 spinal cord (Chai et al. 2014). We confirmed that gene inactivation proceeded as predicted upon Isl1-Cre expression, by comparing Celsr3 mRNA expression by in situ hybridization in control *Isl1-Cre;Celsr3*$^{f/+}$ and *Isl1-Cre;Celsr3*$^{f/-}$ mutant embryos at E13.5. We noted that the global signal was consistently weaker in mutant than in control samples, even in regions such as the cortex or ganglionic eminences that do not express Cre, because only one active allele (*Celsr3*^{f}) is present in mutants, versus 2 (*Celsr3*$^{f/+}$) in controls. In control embryos, *Celsr3* mRNA signal was distributed in postmitotic cells in all cortical fields, the dorsal tier of the ventral telencephalon and the middle region of the IC, as well as in the diencephalon, including the

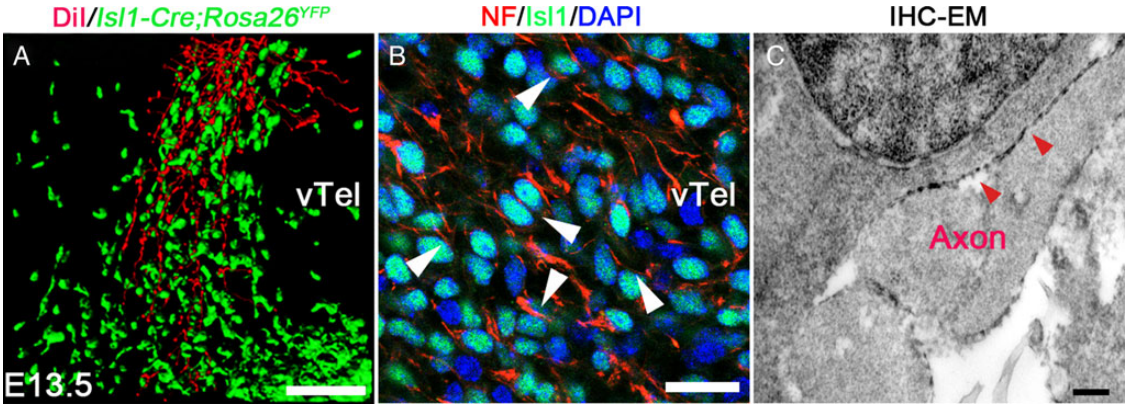

Figure 3. Interactions between growing axons and Isl1-positive cells. (*A*) Confocal stack showing DiI-labeled cortical axons (red) and guidepost cells labeled using *Isl1-Cre;Rosa26*^{YFP} mice (green) in E13.5 ventral telencephalon. Axons ran parallel to one another, in close juxtaposition with YFP-positive cells. (*B* and *C*) Axons (NF-IHC, red) and Isl1-positive cells (green) came in close contact (*B*, arrowheads), which was confirmed by IHC-EM (*C*), where the NF-labeled axon was seen in direct contact (red arrowheads) with the Isl1-positive cell (immunopositive nucleus). Blue in *B* is DAPI; IHC, immunohistochemistry. Scale bars: 50 μm (*A*); 20 μm (*B*); 1 μm (*C*).

hypothalamic anlage, the prethalamus and thalamus (see Supplementary Fig. 4A–C). In contrast, in mutant embryos (see Supplementary Fig. 4D–F), *Celsr3* mRNA was preserved and detected in all cortical fields, ventral telencephalon, hypothalamic anlage and thalamus, though less intense for reasons explained above. Signal was completely absent, however, in the intermediate region of the IC, where the Isl1-positive signal is intense, and in the prethalamus where Isl1 expression is also high (see Fig. 1G). Thus, *Celsr3* mRNA expression was inactivated in the central area of the ventral telencephalon and in prethalamus, consistent with the distribution of Isl1-positive cells described above.

The distribution of axonal bundles was compared in control and *Isl1-Cre;Celsr3*$^{f/-}$ mutant mice using anti-NF immunohistochemistry at E18.5–P0 (Fig. 4). Analysis of 10 mutant animals disclosed some variation in phenotype expressivity. In all of them, a prominent whorl of strongly NF-positive axons was evident at the center of the ventral telencephalon (Fig. 4B, arrow). In 4 out of 10, all thalamic axons were derailed in lateral hypothalamus and subpial telencephalic location (Fig. 4B, arrowhead). The phenotype was slightly less pronounced in the other 6 samples, in which most thalamic axons followed an aberrant ventral path in the telencephalon (see Supplementary Fig. 5G, arrow), whereas others followed a more normal path in the IC (asterisks in Supplementary Fig. 5B,G). This observation of incomplete phenotype expressivity in about half *Isl1-Cre;Celsr3*$^{f/-}$ mutants suggested that Celsr3 may act redundantly with Celsr2, as it does in other contexts (Qu et al. 2010, 2014; Chai et al. 2014). This was assessed by examining *Isl1-Cre;Celsr2*$^{f/-}$*;Celsr3*$^{f/-}$ and *Celsr2*$^{-/-}$*;Isl1-Cre;Celsr3*$^{f/-}$ mice with joint inactivation of Celsr2 and Celsr3. In all those samples, a drastic phenotype was found (see Supplementary Fig. 5C,D,H,I), comparable to the strongest phenotype generated by *Celsr3* inactivation alone, confirming redundancy of Celsr3 and Celsr2. We examined *Isl1-Cre;Fzd3*$^{f/-}$ mice and saw that their IC phenotype was consistently very strong, similar to inactivation of both *Celsr2* and 3 (see Supplementary Fig. 5E,J), in accord with previous observations (Chai et al. 2014; Hua et al. 2014; Qu et al. 2014).

Intriguingly, looping bundles in the middle tier of the IC corridor in *Isl1-Cre;Celsr3*$^{f/-}$ and *Isl1-Cre;Fzd3*$^{f/-}$ were located more medially than those in *Dlx5/6-Cre;Celsr3*$^{f/-}$ mice, where axons stall at the entry of the corridor, at a level facing the LGE (Zhou et al. 2008). To study thalamocortical projections, we implanted DiI crystals in the thalamus and cortex at P0. Upon DiI placement in thalamus in control brains, thalamocortical axons were followed through the IC and reached the cortex (Fig. 4C). By contrast, in mutant brains, whereas some thalamocortical axons followed the same path as in control brains (Fig. 4D, arrow), others were derailed ventrally (Fig. 4D, arrowhead). DiI injection in cortex in control animals labeled fibers along the IC and resulted in retrograde filling of thalamic neurons (Fig. 4E). Similar injections in the mutant cortex filled corticothalamic axons which looped in the IC (Fig. 4F, arrowhead); only a minority progressed to the thalamus where scarce cells were retrogradely labeled (Fig. 4F′). Subcerebral projection axons were traced at P20 using the *Thy1-YFP* transgene (Feng et al. 2000). In contrast to control axons, mutant subcerebral projection axons looped in the IC and a few were misrouted to the thalamus (Fig. 4G,H). Information from vibrissae is relayed by thalamocortical axons to the somatosensory cortex, where they end in cortical barrels (Waite and Cragg 1979). In P7 tangential sections, well-organized barrels were visualized in control brains, whereas barrels were absent or barely defined in mutant samples (Fig. 4I,J). Of note, when atrophic barrels were present in mutants with incomplete phenotype, they were still located at the expected location and layer (Fig. 4K,L). Thus, inactivation of Celsr3 in Isl1-positive cells results in failure of thalamocortical, corticothalamic, and subcerebral axons to progress through the IC.

Pioneer Axons From Prethalamus and Ventral Telencephalon Cross the DTJ in Celsr3/Fzd3-Dependent Manner

We wondered whether Isl1-positive guidepost cells in the ventral telencephalon and prethalamus could send pioneer axons across the DTJ, which would act like a bridge and guide later arriving thalamic and cortical axons. To assess this, we used anti-NF immunostaining, and *Isl1-Cre;Rosa26*^{Tomato} transgenic mice to label Isl1-positive cell bodies and their neurites, at E12.5, before any thalamic or cortical axons reach the DTJ. Fibers originating from Isl1-positive cells were identified by double labeling for NF and the red fluorescent protein. In control embryos, prominent early fibers originating from Isl1-positive cells were seen in the ventral telencephalon and prethalamus, and crossed the DTJ (see Supplementary Fig. 6A–D), forming a bridge. In contrast, in *Isl1-Cre;Celsr3*$^{f/-}$ mutants, many early fibers were tomato-positive and therefore originated from early Isl1-positive cells, yet none crossed the DTJ (see Supplementary Fig. 6E–H). To provide more evidence for such an early bridge, we prepared vibratome

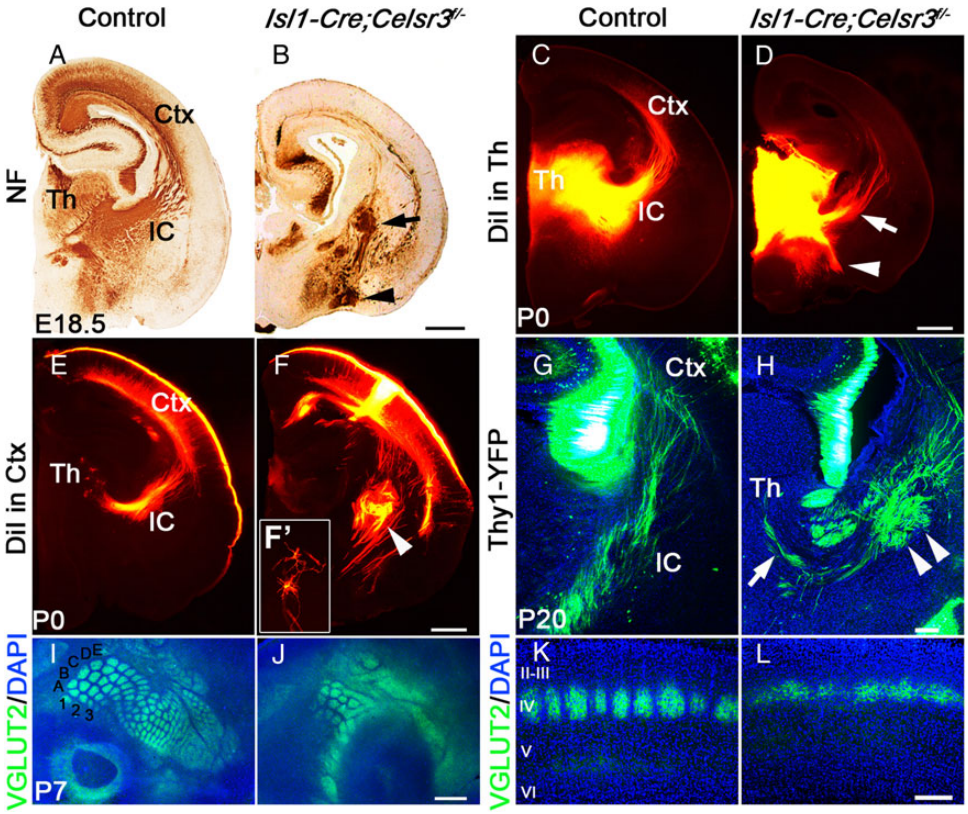

Figure 4. Defective forebrain axonal projections in *Isl1-Cre;Celsr3*$^{f/-}$ mice. (*A* and *B*) E18.5 sections stained by NF antibodies. Unlike in control mice (*A*), in *Isl1-Cre;Celsr3*$^{f/-}$ mutant mice (*B*), fibers looped aberrantly in the middle area of the ventral telencephalon (arrow) and were misrouted at the level of the DTJ (arrowhead). (*C–F*) DiI tracing at P0. Upon DiI injection in thalamus (Th), unlike in control brain (*C*), in mutants, only a minority of thalamic axons followed a normal path (*D*, arrow) and many were misrouted ventrally (*D*, arrowhead). Upon DiI injection in cortex (Ctx), cortical axons traversed the internal capsule (IC) in the control (*E*) and retrogradely labeled neurons were seen in thalamus. In contrast, in *Isl1-Cre;Celsr3*$^{f/-}$ mice, cortical axons stalled and formed whorls (*F*, arrowhead), and rare thalamic neurons were labeled (*F'*). (*G* and *H*) Unlike control axons (*G*), mutant corticospinal axons (*H*), traced using *Thy1-YFP* at P20, formed whorls in the IC (arrowheads), and some projected aberrantly to thalamus (arrow). (*I–L*) Cortical barrels in P7 tangential and coronal sections stained with anti-VGLUT2. In the control, barrels were well organized (*I* and *K*). In mutants with partial phenotype (*J* and *L*), barrels were blurry although a few were visible and their anatomical localization was preserved. Scale bars: 500 μm (*A–F* and *I–J*); 200 μm (*G–H* and *K–L*).

sections at E12.5 in an oblique orientation to include prethalamus and ventral telencephalon (Fig. 5A), and used 2-photon imaging and tridimensional reconstruction to analyze the region of the DTJ. Isl1-positive cells and their neurites were labeled using the *Rosa26*^{Tomato} transgene. In control samples ($n = 11$), fluorescent fibers joining the prethalamus and ventral telencephalon across the DTJ were clearly visualized (Fig. 5B, arrows; see Supplementary Movie 1). At later stages, E15.5 and P0, fiber bundles in the region increased in size due to addition of thalamocortical and corticothalamic fibers, among which early axons from the bridge appeared to subsist (Fig. 5G,H). In *Isl1-Cre;Celsr3*$^{f/-}$ mutants ($n = 19$), the bridge was completely absent in 14 samples (Fig. 5C,F; see Supplementary Movie 2), and partial (defined by a few fibers crossing the DTJ) in 5 samples (Fig. 5D, arrowheads, F). No bridge was found in any *Isl1-Cre;Fzd3*$^{f/-}$ mutant ($n = 5$, Fig. 5E,F).

To confirm that Isl1-positive cells in ventral telencephalon and prethalamus sent pioneer axons across the DTJ, we implanted small NeuroVue filter fragments in E12.5 vibratome slices (600-μm thickness) prepared from mutant (*Isl1-Cre;Celsr3*$^{f/-}$; *Rosa26*^{Tomato}) and control (*Isl1-Cre;Rosa26*^{Tomato}) embryos. When NeuroVue was inserted in the prethalamus in control slices ($n = 11$), Isl1-positive cell bodies (78.82 ± 11.16 cells/sample) were retrogradely labeled in the ventral telencephalon (Fig. 6A,B,B′,E). Among 5 mutant samples, no retrogradely labeled cell bodies were seen in 4, and 17 retrogradely labeled cells were seen in one (Fig. 6C,C′,D,E). Reciprocally, upon NeuroVue insertion in the control ventral telencephalon ($n = 10$), Isl1-positive cell bodies (59.20 ± 11.60 cells/sample) were retrogradely labeled in the prethalamus (Fig. 6F,G,G′,J). However, only one mutant embryo showed very few labeled cells (10 cells per sample) and no cell bodies were retrogradely labeled in 4 other mutant samples (Fig. 6H,H′,I,J). Those tracing experiments show that Isl1-positive cells in the ventral medial telencephalon and in the prethalamus contribute pioneer axons to the bridge in both directions, across the DTJ. We also carried out DiI labeling experiments by placing tracer in the prethalamus in E12.5 *Dlx5/6-Cre;Celsr3*$^{f/+}$ (control) and *Dlx5/6-Cre;Celsr3*$^{f/-}$ (mutant) embryos, combined with visualization of EGFP and Isl1 IHC to identify retrogradely labeled Dlx and Isl1 guideposts, respectively. Among retrogradely labeled cells in the ventral telencephalon, some were double positive for Dlx5/6 and Isl1, and some were only Isl1-positive (see Supplementary Fig. 7A,B,F), in accord with the partial colocalization (see Supplementary Fig. 1). In nice *Dlx5/6-Cre;Celsr3*$^{f/-}$ mutants, no retrogradely cells were found in 6 and only a few cells were found in 3 embryos (see Supplementary Fig. 7C,D,E,F), confirming that Dlx5/6 and Isl1-positive guideposts in ventral telencephalon both contribute to the early scaffold across the DTJ.

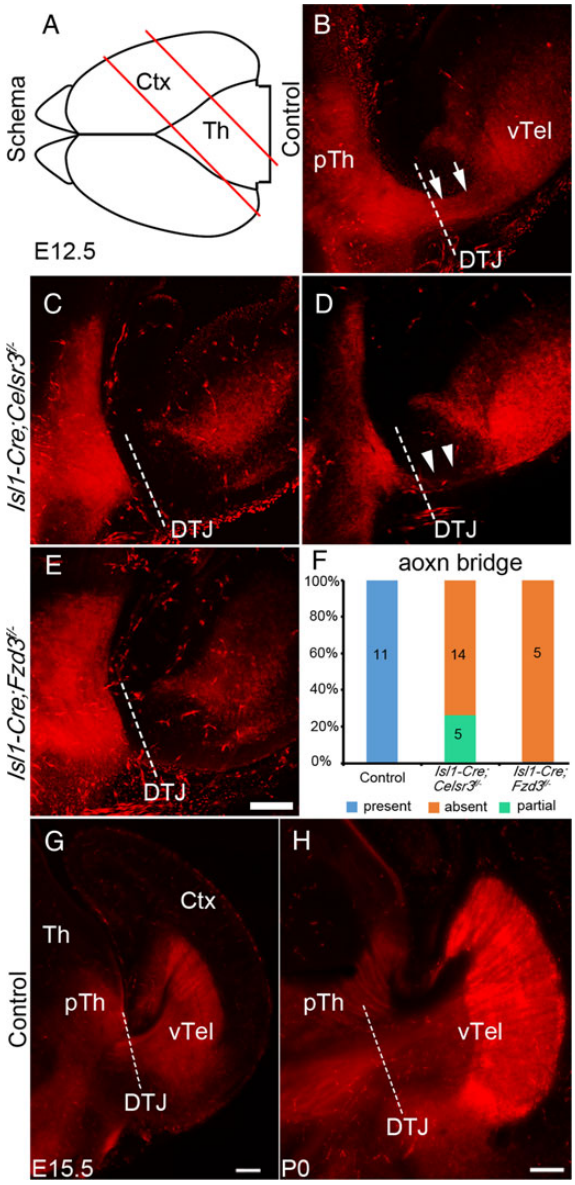

Figure 5. The early scaffold "bridge" between the ventral telencephalon and the prethalamus. (*A*) Schema illustrating the preparation of oblique slices. (*B–E*) Merged stacks of sections generated by 2-photon microscopy, using E12.5 *Isl1-Cre;Rosa26*^{Tomato} mice to label Isl1-positive cells and fibers in control (*B*), *Isl1-Cre;Celsr3*$^{f/-}$ (C and *D*) and *Isl1-Cre;Fzd3*$^{f/-}$ embryos (*E*) at E12.5. In all control embryos, a connecting "bridge" (*B*, arrows) was evident across the DTJ (interrupted line), between ventral telencephalon (vTel) and prethalamus (pTh). The bridge was completely absent in 14 *Isl1-Cre;Celsr3*$^{f/-}$ samples (*C*), and partial in 5 other *Isl1-Cre;Celsr3*$^{f/-}$ samples (*D*, arrowheads) The bridge was fully absent in all *Isl1-Cre;Fzd3*$^{f/-}$ samples (*E*). (*F*) Summary histogram. (*G* and *H*) Axon bundles from Isl1-positive cells crossing the DTJ were visualized in sections of E15.5 (*G*) and P0 *Isl1-Cre;Rosa26*^{Tomato} embryos. Ctx, cortex; Th, thalamus. Scale bars: 50 μm (*B–E*); 200 μm (*G* and *H*).

The bridge was formed by pioneer fibers among which a few cells with features of migrating cells appeared dispersed, as indicated by NF immunostaining of E12.5 *Isl1-Cre;Rosa26*^{Tomato} embryos (Fig. 7*A*,*B*). To understand this better, we injected cell tracker green in prethalamus and ventral telencephalon in oblique slices at E12.5, and cultured slices for 2 days to trace putative migrating cells. As shown in Figure 7*C–F*, tracer injection in the prethalamus and the ventral telencephalon resulted in labeling of sparse cells in the ventral telencephalon and the prethalamus, repectively.

Thalamocortical Axons Progress on the Early Bridge Constructed by Isl1 Cells

To study the relationship of thalamocortical axons and the bridge, we implanted NeuroVue into the dorsal thalamus to trace thalamocortical axons in mutant (*Isl1-Cre;Celsr3*$^{f/-}$*;Rosa26*^{Tomato}) and control (*Isl1-Cre;Rosa26*^{Tomato}) embryos at E13.5, the stage when the first axons from the thalamus cross the DTJ. In control samples ($n = 12$), a well-defined bundle of thalamocortical axons (Fig. 8*A*,*B*, green arrowheads) was seen at the dorsal aspect and in close contact with the bridge (Fig. 8*A*,*B*, red arrowheads), crossing the DTJ and reaching the ventral telencephalon directly. In 2 out of 10 mutant embryos, a few fibers crossed the DTJ in contact with very thin bridges (Fig. 8*C*,*F*); furthermore those axons ran erratically in the ventral telencephalon after crossing the DTJ (Fig. 8*D*, arrowheads). No thalamocortical axons crossed the DTJ in 8 other samples in which the bridge was completely absent (Fig. 8*E*,*F*).

Altogether, our data demonstrate that Celsr3 and Fzd3 are required for establishment of early reciprocal projections between Isl1-positive cells in medial ventral telencephalon and prethalamus. Those pioneer projections form an early bridge that provides a substrate and assists the progression of thalamic axons that begin to cross the DTJ one day later.

Discussion

This study shows that expression of Celsr3 and Fzd3 in 2 early populations of Isl1-positive neurons, one in the ventral telencephalon and another one in prethalamus, is required to steer cortical axons in the IC corridor, and thalamic axons through the DTJ (Schema in Fig. 9).

Together with previous observations using *Dlx5/6-Cre* inactivation (Zhou et al. 2008), the present data show that, depending on which guidepost cell is lacking Celsr3 or Fzd3, corticofugal axons stall at different levels in the IC corridor. Inasmuch as corticothalamic axons grow normally in mice with inactivation of *Celsr3* or *Fzd3* in the cortical anlage (Zhou et al. 2008), the role of Celsr3 and Fzd3 in that context is therefore noncortical cell autonomous, in that both proteins are required in guidepost cells but not in cortical neurons of origin (Hua et al. 2014; Qu et al. 2014) . This suggests a model in which Celsr3 and Fzd3, as well as probably Linx (Mandai et al. 2014) act on cortical axons indirectly, by instructing the formation of an early permissive corridor in the ventral telencephalon, composed of Isl1-positive and other guidepost cells, which at that early stage are local pioneer neurons and their axons (Fig. 9*A*). Regional gene inactivation upon expression of Cre in different segments of that early scaffold may result in stalling of cortical axons at the corresponding defective segments (Fig. 9*B–D*). Intriguingly, the axon balling in the IC corridor generated by inactivation of *Celsr3* or *Fzd3* upon *Dlx5/6* or *Isl1-Cre* expression is never found when inactivation is driven by *Foxg1-Cre*, which is expressed more widely than *Dlx5/6* or *Isl1*, in ventral as well as dorsal telencephalon (Zhou et al. 2008). This fits in nicely with the known role of early cortical preplate pioneer axons in steering corticothalamic projections (McConnell et al. 1989). Celsr3 and Fzd3 could mediate reciprocal interactions among early neurons in preplate and ventral telencephalon and their axons across the PSPB. This might be analogous to the reciprocal projections that form the bridge at the DTJ (discussed below), even though a clearly defined anatomical

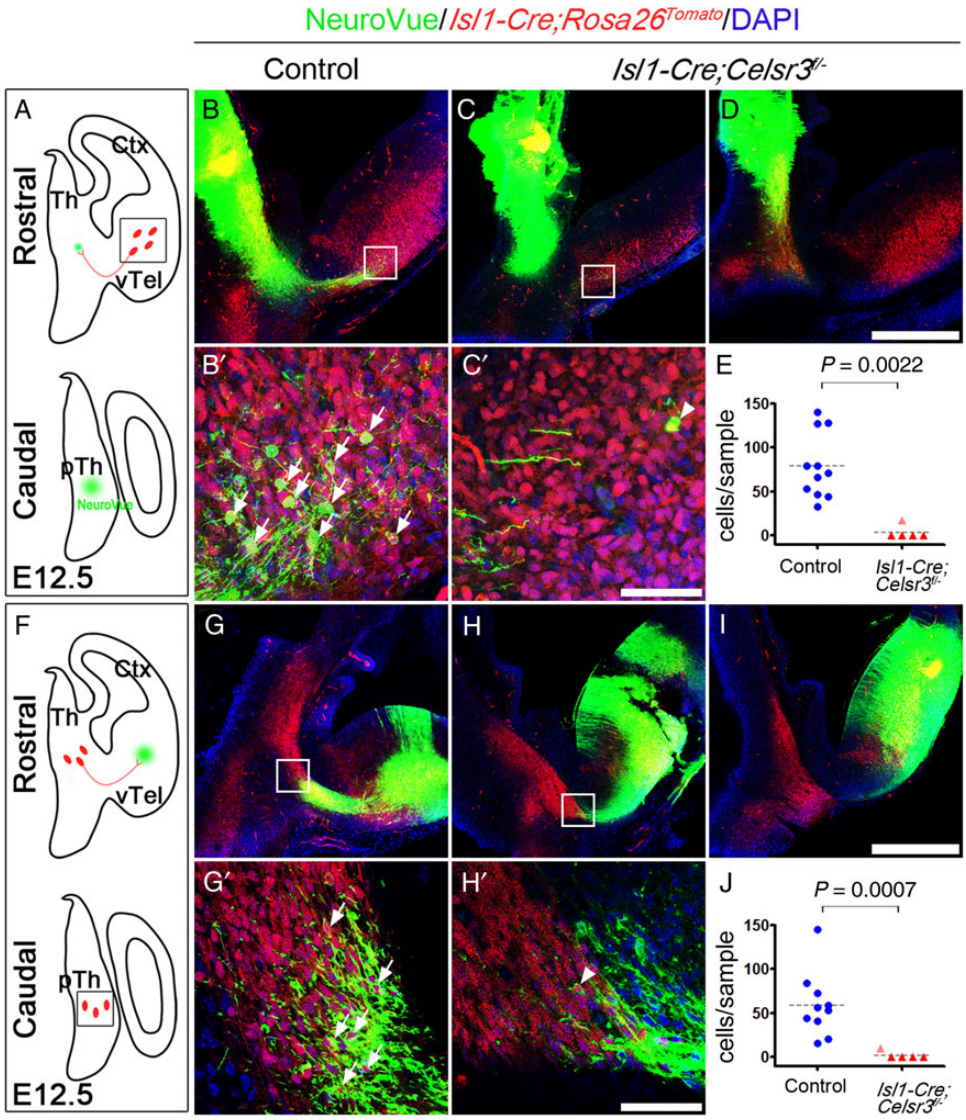

Figure 6. Early reciprocal pioneer projections between ventral telencephalon and prethalamus. NeuroVue was inserted in E12.5 vibratome slices. Isl1-positive cells were detected using the *Isl1-Cre;Rosa26*^{Tomato} transgene (red), and DAPI (blue) was used as a general nuclear stain. (*A–D*) Upon NeuroVue implantation in prethalamus (*A*), many Isl1-positive cells were back labeled in the ventral telencephalon in control (*B* and *B′*, arrows), a few in one mutant (*C* and *C′*, arrowhead) and none in 4 other mutants (*D*). (*E*) Summary of results; $P = 0.0022$ (Mann–Whitney *U* test). (*F–I*) NeuroVue implantation in ventral telencephalon (*F*) resulted in retrograde labeling of many Isl1-positive cells in the prethalamus in control (*G* and *G′*, arrows), a few in one mutant (*H* and *H′*, arrowhead) and none in 4 other mutant embryos (*I*). (*J*) Summary of results; $P = 0.0007$ (Mann–Whitney *U* test). (*B′*, *C′*, *G′*, and *H′*) are higher magnification of boxed areas in (*B*, *C*, *G*, and *H*), respectively. pTh: prethalamus; Ctx, cortex; vTel, ventral telencephalon; Th, thalamus. Scale bars: 400 μm (*B–D* and *G–I*); 50 μm (*B′*, *C′*, *G′*, and *H′*).

bridge is not found at the PSPB, presumably because projections that cross that boundary are more widely dispersed and do not form as clearly defined a bundle as those that cross the DTJ (Lopez-Bendito et al. 2006; Molnar et al. 2012; Deck et al. 2013).

DTJ crossing requires Celsr3, Fzd3, and Linx (Wang et al. 2002; Tissir et al. 2005; Mandai et al. 2014). Celsr3 and Fzd3 are not required in thalamic axons themselves, but are crucial in guidepost cells (Qu et al. 2014). Our results identify those cells as p3-derived, Pax6- and Isl1-expressing cells, different than calretinin-positive cells from the thalamic eminence and Reln-expressing cells in reticular thalamus. Those data are in agreement with observations that: (1) Inactivation of Fzd3 upon Calretinin-Cre expression fails to generate any thalamic fiber misrouting (Hua et al. 2014); (2) The expression and function of Pax6 in prethalamus is required for thalamic axon navigation (Jones et al. 2002; Simpson et al. 2009); and (3) The Olig2 transcription factor, which is expressed in the ventricular zone of p3, regulates prethalamus formation and is crucial for thalamic fiber progression through prethalamus, and for DTJ crossing (Vue et al. 2007; Inamura et al. 2011; Ono et al. 2014).

Early pioneer axons emanating from Isl1-positive cells in medioventral basal forebrain and prethalamus cross the DTJ in both directions and a few Isl1-positive cells migrate among them from both directions. The early bridge formed by Isl1-positive pioneer cells and axons is followed by developing thalamic axons when they grow toward ventral telencephalon. This bridge cannot form in *Celsr3* and *Fzd3* mutant mice, and this presumably explains why thalamic fibers fail to turn and cross the DTJ

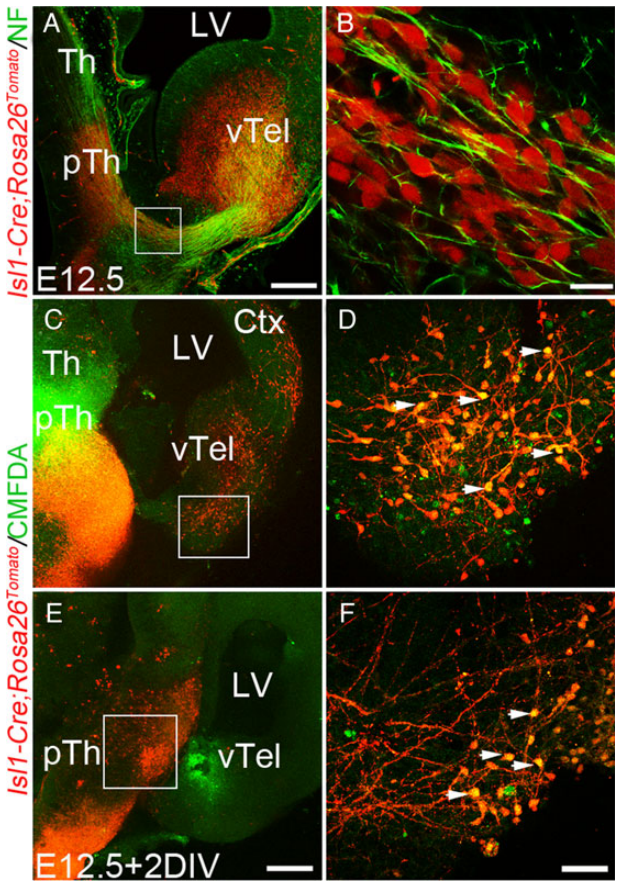

Figure 7. Isl1-positive cells reciprocally migrate across the DTJ from the prethalamus and ventral telencephalon. (*A* and *B*) The early scaffold bridge is composed of Isl1-positive fibers and migrating cells disclosed using anti-neurofilament (NF) IHC and *Isl1-Cre;Rosa26*^{Tomato} tracing. Oblique section at E12.5, with Isl1-positive cells revealed using the Tomato transgene, and axons stained with anti-neurofilaments (green) (*A*).The selected area from the scafold bridge in A contained both yellow fibers and red cells (*B*). (*C*–*F*) In E12.5 oblique sections from *Isl1-Cre;Rosa26*^{Tomato} embryos, CMFDA (green) was placed into the prethalamus (*C*) or the ventral telencephalon (*E*), and slices were cultured for 2 days (2DIV). Isl1-positive cells were red due to Tomato fluorescence. Double labeled cells could be seen in both ventral telencephalon (arrows in *D*) and prethalamus (arrows in *F*). (*D* and *F*) are selected areas from (*C* and *E*), respectively. pTh, prethalamus; Ctx, cortex; vTel, ventral telencephalon; Th, thalamus; LV, lateral ventricle. Scale bars: 200 μm (*A*, *C*, and *E*); 20 μm (*B*); 50 μm (*D*, *F*).

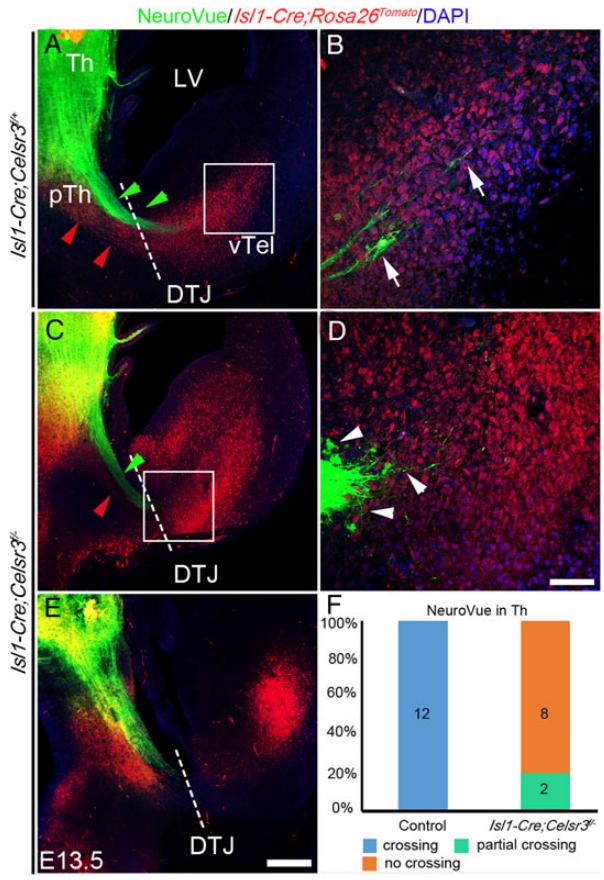

Figure 8. The bridge is required for thalamocortical axons to cross the DTJ from E13.5. Early thalamocortical axons were labeled at E13.5, following NeuroVue implantation in the dorsal thalamus, and Isl1-positive cells were visualized by the *Isl1-Cre;Rosa26*^{Tomato} transgene, in oblique slices. (*A* and *B*) In control embryos, thalamocortical axons (*A*, green arrowheads) followed the bridge (*A*, red arrowheads) to cross the DTJ (*A*) and then ran in the ventral telencephalon uniformly (*B*, arrows). (*C*–*F*) In 2 mutants, a few thalamocortical fibers (*C*, green arrowhead) could cross the DTJ along a partial bridge (*C*, red arrowhead) and then ran randomly in the ventral telencephalon (*D*, arrowheads). No thalamocortical axons crossed the DTJ in 8 other mutant embryos with the absence of the bridge (*E*). (*F*) Summary histogram. (*B* and *D*) are higher magnification of selected areas in (*A* and *C*) respectively. Th, dorsal thalamus; LV, lateral ventricle; pTh, prethalamus; vTel, ventral telencephalon. Scale bars: 200 μm (*A*, *C*, *E*); 50 μm (*B*, *D*).

in those mutants and possibly other mutants with similar phenotypes. At later developmental stages, some pioneer Isl1 ventral telencphalic guidepost cells differentiate into cholinergic neurons and their axons might be incorporated and diluted among GABAergic pallidothalamic fibers, whose development remains poorly understood (Metin and Godement 1996; Molnar and Cordery 1999; Ehrman et al. 2013; Jia et al. 2014). This is reminiscent of cortical subplate cells, which serve as guideposts and later become deep layer 6b neurons. Like for Isl1 guideposts, whether some subplate cells commit apoptosis after serving their guidepost function remains quite controversial (Hoerder-Suabedissen and Molnar 2013).

Our observations lead us to propose that Celsr3, Fzd3 and possibly Linx preside over the formation of an early scaffold made of pioneer neurons and their axons. This guidepost scaffold encompasses the bridge across the DTJ, the corridor in the ventral telencephalon, and early axons from ventral telencephalon and cortical preplate that cross the PSPB (McConnell et al. 1989; Hoerder-Suabedissen and Molnar 2015). Although molecular mechanism remain to be elucidated, it is tempting to consider a model inspired by Wnt-signaling complexes, which include, in addition to Frizzled receptors, 7 pass adhesion G-protein coupled receptors (GPR) such as GPR124 (Zhou and Nathans 2014), and Lrp5/6 transmembrane proteins (Tamai et al. 2000; Wehrli et al. 2000). Available data, particularly on conditional inactivation phenotypes, are compatible with the following hypothetical mechanism: 1) Fzd3 could impart directional information by reading gradients of diffusible ligands such as Wnt; (2) Homophilic interactions between Celsr3 cadherins, which belong to the family of adhesion GPR, would promote adhesion among guidepost neurons and/or their axons; and (3) Linx could act as an essential structural component of the Celsr3/Fzd3 complex, like Lrp5/6 in canonical Wnt-signaling complexes.

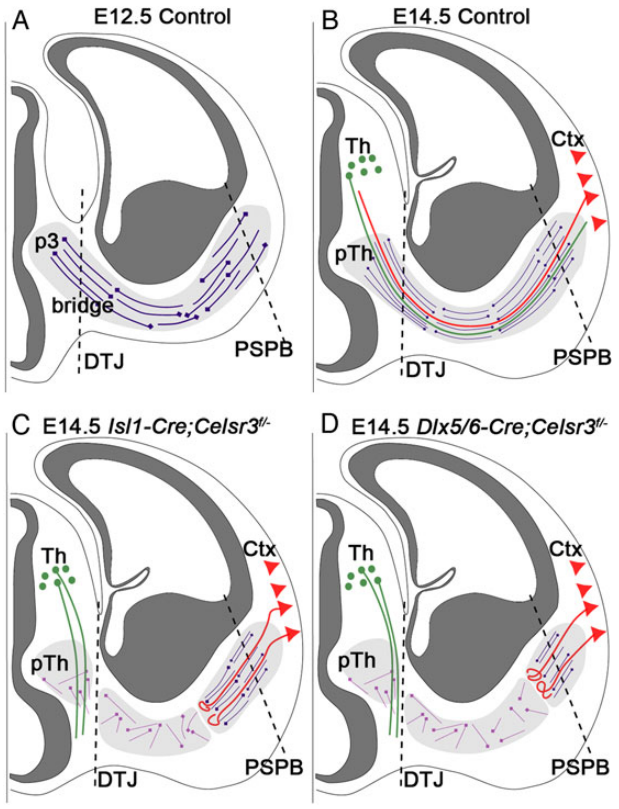

Figure 9. Summary of defective axonal bundles in *Isl1-Cre;Celsr3*$^{f/-}$ mice. (*A*) In control embryos at E12.5, prior to growth of thalamic and cortical axons, Isl1-positive cells (dark mauve) form an early scaffold that extends from prosomere 3 (p3), across the DTJ, in ventral telencephalon, and across the PSPB to subcortex (light gray area). Reciprocal projections across the diencephalon–telencephalon junction (DTJ) form a "bridge" which is absent in Celsr3 and Fzd3 mutant embryos. Dark gray: ventricular zones. (*B–D*) At later stages, for example, E14.5, thalamocortical (green) and corticothalamic (red) axons extend in the corridor in vTel (light gray) and reach their respective targets in control mice (*B*). In *Isl1-Cre;Celsr3*$^{f/-}$ mice (*C*), the early scaffold is disorganized in regions of Isl1 expression (light mauve cells). Thalamocortical axons (green) are misrouted ventrally, and corticothalamic axons (red) stall and form a whorl in the corridor, more medially than in *Dlx5/6-Cre;Celsr3*$^{f/-}$ mutants (*D*). Ctx, cortex; pTh, prethalamus; Th, thalamus; DTJ, diencephalon–telencephalon junction; PSPB, pallium–subpallium boundary.

Supplementary material

Supplementary material can be found at: http://www.cercor.oxfordjournals.org/.

Funding

This work was supported by the following grants: National Natural Science Foundation of China (31070955, 31200826), National Basic Research Program of China (973 Program, 2014CB542205), Project of Internation as well as Hong Kong, Macao & Taiwan Science and Technology Cooperation Innovation Platform in Universities in Guangdong Province (2013gjhz0002), Programme of Introducing Talents of Discipline to Universities (B14036), Science & Technology Planning and Key Technology Innovation Projects of Guangdong (2014B050504006), Health and Medical Collaborative Innovation Major Projects of Guangzhou (201400000003-2), and by Belgian grants FNRS PDR T0002, Welbio CR-2012-007, IAP "Wibrain" P7/20 from Belspo to A.M.G. Funding to pay the Open Access publication charges for this article was provided by National Natural Science Foundation of China (31070955, 31200826).

Notes

We wish to thank K. Campbell for Dlx5/6-Cre mice and Fadel Tissir for critical comments. *Conflict of Interest*: None declared.

References

Abbott LC, Jacobowitz DM. 1999. Developmental expression of calretinin-immunoreactivity in the thalamic eminence of the fetal mouse. Int J Dev Neurosci. 17:331–345.

Bielle F, Marcos-Mondejar P, Keita M, Mailhes C, Verney C, Nguyen Ba-Charvet K, Tessier-Lavigne M, Lopez-Bendito G, Garel S. 2011. Slit2 activity in the migration of guidepost neurons shapes thalamic projections during development and evolution. Neuron. 69:1085–1098.

Caballero IM, Manuel MN, Molinek M, Quintana-Urzainqui I, Mi D, Shimogori T, Price DJ. 2014. Cell-autonomous repression of shh by transcription factor pax6 regulates diencephalic patterning by controlling the central diencephalic organizer. Cell Rep. 8:1405–1418.

Chai G, Zhou L, Manto M, Helmbacher F, Clotman F, Goffinet AM, Tissir F. 2014. Celsr3 is required in motor neurons to steer their axons in the hindlimb. Nat Neurosci. 17:1171–1179.

Cohen NR, Taylor JS, Scott LB, Guillery RW, Soriano P, Furley AJ. 1998. Errors in corticospinal axon guidance in mice lacking the neural cell adhesion molecule L1. Curr Biol. 8:26–33.

Corbin JG, Rutlin M, Gaiano N, Fishell G. 2003. Combinatorial function of the homeodomain proteins Nkx2.1 and Gsh2 in ventral telencephalic patterning. Development. 130: 4895–4906.

Deck M, Lokmane L, Chauvet S, Mailhes C, Keita M, Niquille M, Yoshida M, Yoshida Y, Lebrand C, Mann F, et al. 2013. Pathfinding of corticothalamic axons relies on a rendezvous with thalamic projections. Neuron. 77:472–484.

Dottori M, Hartley L, Galea M, Paxinos G, Polizzotto M, Kilpatrick T, Bartlett PF, Murphy M, Kontgen F, Boyd AW. 1998. EphA4 (Sek1) receptor tyrosine kinase is required for the development of the corticospinal tract. Proc Natl Acad Sci U S A. 95:13248–13253.

Ehrman LA, Mu X, Waclaw RR, Yoshida Y, Vorhees CV, Klein WH, Campbell K. 2013. The LIM homeobox gene Isl1 is required for the correct development of the striatonigral pathway in the mouse. Proc Natl Acad Sci U S A. 110:E4026–E4035.

Feng G, Mellor RH, Bernstein M, Keller-Peck C, Nguyen QT, Wallace M, Nerbonne JM, Lichtman JW, Sanes JR. 2000. Imaging neuronal subsets in transgenic mice expressing multiple spectral variants of GFP. Neuron. 28:41–51.

Greig LC, Woodworth MB, Galazo MJ, Padmanabhan H, Macklis JD. 2013. Molecular logic of neocortical projection neuron specification, development and diversity. Nat Rev Neurosci. 14:755–769.

Hevner RF, Miyashita-Lin E, Rubenstein JL. 2002. Cortical and thalamic axon pathfinding defects in Tbr1, Gbx2, and Pax6 mutant mice: evidence that cortical and thalamic axons interact and guide each other. J Comp Neurol. 447:8–17.

Hoerder-Suabedissen A, Molnar Z. 2013. Molecular diversity of early-born subplate neurons. Cereb Cortex. 23:1473–1483.

Hoerder-Suabedissen A, Molnar Z. 2015. Development, evolution and pathology of neocortical subplate neurons. Nat Rev Neurosci. 16:133–146.

Hua ZL, Jeon S, Caterina MJ, Nathans J. 2014. Frizzled3 is required for the development of multiple axon tracts in the mouse central nervous system. Proc Natl Acad Sci U S A. 111: E3005–E3014.

Inamura N, Ono K, Takebayashi H, Zalc B, Ikenaka K. 2011. Olig2 lineage cells generate GABAergic neurons in the prethalamic nuclei, including the zona incerta, ventral lateral geniculate nucleus and reticular thalamic nucleus. Dev Neurosci. 33:118–129.

Jia Z, Guo Y, Tang Y, Xu Q, Li B, Wu Q. 2014. Regulation of the protocadherin Celsr3 gene and its role in globus pallidus development and connectivity. Mol Cell Biol. 34:3895–3910.

Jones L, Lopez-Bendito G, Gruss P, Stoykova A, Molnar Z. 2002. Pax6 is required for the normal development of the forebrain axonal connections. Development. 129:5041–5052.

Liu Y, Shi J, Lu CC, Wang ZB, Lyuksyutova AI, Song XJ, Zou Y. 2005. Ryk-mediated Wnt repulsion regulates posterior-directed growth of corticospinal tract. Nat Neurosci. 8:1151–1159.

Lopez-Bendito G, Cautinat A, Sanchez JA, Bielle F, Flames N, Garratt AN, Talmage DA, Role LW, Charnay P, Marin O, et al. 2006. Tangential neuronal migration controls axon guidance: a role for neuregulin-1 in thalamocortical axon navigation. Cell. 125:127–142.

Lopez-Bendito G, Molnar Z. 2003. Thalamocortical development: how are we going to get there? Nat Rev Neurosci. 4:276–289.

Mandai K, Reimert DV, Ginty DD. 2014. Linx mediates interaxonal interactions and formation of the internal capsule. Neuron. 83:93–103.

McConnell SK, Ghosh A, Shatz CJ. 1989. Subplate neurons pioneer the first axon pathway from the cerebral cortex. Science. 245:978–982.

Metin C, Godement P. 1996. The ganglionic eminence may be an intermediate target for corticofugal and thalamocortical axons. J Neurosci. 16:3219–3235.

Molnar Z, Blakemore C. 1991. Lack of regional specificity for connections formed between thalamus and cortex in coculture. Nature. 351:475–477.

Molnar Z, Cordery P. 1999. Connections between cells of the internal capsule, thalamus, and cerebral cortex in embryonic rat. J Comp Neurol. 413:1–25.

Molnar Z, Garel S, Lopez-Bendito G, Maness P, Price DJ. 2012. Mechanisms controlling the guidance of thalamocortical axons through the embryonic forebrain. Eur J Neurosci. 35:1573–1585.

Ono K, Clavairoly A, Nomura T, Gotoh H, Uno A, Armant O, Takebayashi H, Zhang Q, Shimamura K, Itohara S, et al. 2014. Development of the prethalamus is crucial for thalamocortical projection formation and is regulated by Olig2. Development. 141:2075–2084.

Ozdinler PH, Macklis JD. 2006. IGF-I specifically enhances axon outgrowth of corticospinal motor neurons. Nat Neurosci. 9:1371–1381.

Qu Y, Glasco DM, Zhou L, Sawant A, Ravni A, Fritzsch B, Damrau C, Murdoch JN, Evans S, Pfaff SL, et al. 2010. Atypical cadherins Celsr1–3 differentially regulate migration of facial branchiomotor neurons in mice. J Neurosci. 30:9392–9401.

Qu Y, Huang Y, Feng J, Alvarez-Bolado G, Grove EA, Yang Y, Tissir F, Zhou L, Goffinet AM. 2014. Genetic evidence that Celsr3 and Celsr2, together with Fzd3, regulate forebrain wiring in a Vangl-independent manner. Proc Natl Acad Sci U S A. 111:E2996–E3004.

Schiffmann SN, Bernier B, Goffinet AM. 1997. Reelin mRNA expression during mouse brain development. Eur J Neurosci. 9:1055–1071.

Scholpp S, Lumsden A. 2010. Building a bridal chamber: development of the thalamus. Trends Neurosci. 33:373–380.

Sherman SM, Guillery RW. 2011. Distinct functions for direct and transthalamic corticocortical connections. J Neurophysiol. 106:1068–1077.

Simpson TI, Pratt T, Mason JO, Price DJ. 2009. Normal ventral telencephalic expression of Pax6 is required for normal development of thalamocortical axons in embryonic mice. Neural Dev. 4:19.

Stenman J, Toresson H, Campbell K. 2003. Identification of two distinct progenitor populations in the lateral ganglionic eminence: implications for striatal and olfactory bulb neurogenesis. J Neurosci. 23:167–174.

Tamai K, Semenov M, Kato Y, Spokony R, Liu C, Katsuyama Y, Hess F, Saint-Jeannet JP, He X. 2000. LDL-receptor-related proteins in Wnt signal transduction. Nature. 407:530–535.

Tessier-Lavigne M. 2002. Wiring the brain: the logic and molecular mechanisms of axon guidance and regeneration. Harvey Lect. 98:103–143.

Tissir F, Bar I, Jossin Y, De Backer O, Goffinet AM. 2005. Protocadherin Celsr3 is crucial in axonal tract development. Nat Neurosci. 8:451–457.

Tissir F, Goffinet AM. 2013. Shaping the nervous system: role of the core planar cell polarity genes. Nat Rev Neurosci. 14:525–535.

Tissir F, Wang CE, Goffinet AM. 2004. Expression of the chemokine receptor Cxcr4 mRNA during mouse brain development. Brain Res Dev Brain Res. 149:63–71.

Vue TY, Aaker J, Taniguchi A, Kazemzadeh C, Skidmore JM, Martin DM, Martin JF, Treier M, Nakagawa Y. 2007. Characterization of progenitor domains in the developing mouse thalamus. J Comp Neurol. 505:73–91.

Waite PM, Cragg BG. 1979. The effect of destroying the whisker follicles in mice on the sensory nerve, the thalamocortical radiation and cortical barrel development. Proc R Soc Lond B Biol Sci. 204:41–55.

Wang Y, Thekdi N, Smallwood PM, Macke JP, Nathans J. 2002. Frizzled-3 is required for the development of major fiber tracts in the rostral CNS. J Neurosci. 22:8563–8573.

Wehrli M, Dougan ST, Caldwell K, O'Keefe L, Schwartz S, Vaizel-Ohayon D, Schejter E, Tomlinson A, DiNardo S. 2000. arrow encodes an LDL-receptor-related protein essential for Wingless signalling. Nature. 407:527–530.

Zhou L, Bar I, Achouri Y, Campbell K, De Backer O, Hebert JM, Jones K, Kessaris N, de Rouvroit CL, O'Leary D, et al. 2008. Early forebrain wiring: genetic dissection using conditional Celsr3 mutant mice. Science. 320:946–949.

Zhou L, Jossin Y, Goffinet AM. 2007. Identification of small molecules that interfere with radial neuronal migration and early cortical plate development. Cereb Cortex. 17:211–220.

Zhou Y, Nathans J. 2014. Gpr124 controls CNS angiogenesis and blood-brain barrier integrity by promoting ligand-specific canonical wnt signaling. Dev Cell. 31:248–256.